Computational Modelling of Concrete and Concrete Structures – Meschke, Pichler & Rots (Eds)

Application of NLFEA for crack width calculations in SLS

O. Terjesen
Department of Structural Engineering, University of Agder, Norway

T. Kanstad & R. Tan
Department of Structural Engineering, Norwegian University of Science and Technology, Norway

ABSTRACT: In this paper, computer-based simulation is carried out using the Finite Element Analysis (FEA) package Abaqus to study crack widths in reinforced concrete beams. A set of experimentally tested beams are investigated, and measured crack widths are compared with crack widths predicted by nonlinear FEA (NLFEA) and relevant design codes. It is shown that Eurocode 2 (EC2), fib Model Code 2010 (MC2010) and the draft for new EC2 underestimates the crack widths at the outermost concrete face to different extents while they are conservative at reinforcement level. Crack widths predicted by NLFEA, on the other hand, provides good crack width predictions at the outermost concrete face for both investigated beams.

1 INTRODUCTION

Crack widths in concrete structures should be limited due to aesthetics, durability, and functional requirements (e.g., tightness). Although research related to this topic has been ongoing since modern time, large uncertainties and large need for further research remains. The large uncertainties are especially due to large scale concrete structures, the large concrete covers applied for structures in harsh environments, and introduction of more eco-friendly modern concretes (Basteskår et al. 2018). Strict crack width limits lead to increased amount of reinforcement and the economic consequences are proven to be large (Basteskår et al. 2019).

The work presented is part of the PhD-project of the first author and are related to the large research activity funded by the large Norwegian infrastructure project "Ferry-free E39" and the PhD work of Reignard Tan (Tan, Reignard 2019).

The main objective of this paper is to investigate how nonlinear finite element analysis (NLFEA) can be applied to predict maximum crackwidths, which furthermore are compared to crack widths predicted by analytical calculation methods in design codes such as Eurocode 2 (EC2) and *fib* Model Code 2010 (MC2010). The study is benchmarked against the experimental results from the comprehensive and well documented beam tests of Hognestad (1962).

2 CONCRETE DAMAGE PLASTICITY

The Concrete Damage Plasticity (CDP) model is a continuum, plasticity-based, damage model for concrete and is in Abaqus based on the models proposed by Lubliner et al. (1989) and by Lee and Fenves (1998). It is assumed that the two main failure mechanisms are tensile cracking and compressive crushing of the concrete material. The evolution of the yield (or failure) surface is controlled by two hardening variables in tension (ε_t^{pl}) and compression (ε_p^{pl}), linked to the respective failure mechanisms.

The experimental behaviour of reinforced concrete beams cannot be captured by elastic damage models or elastic-plastic constitutive laws only. Because in such models irreversible strains cannot be captured. In Figure 1b it can be noticed that a zero stress corresponds to a zero strain which makes the damage value underestimated. On the other hand, when an elastic plastic relation is adopted, the strain will be overestimated since the unloading curve will follow the elastic slope as shown in Figure 1c.

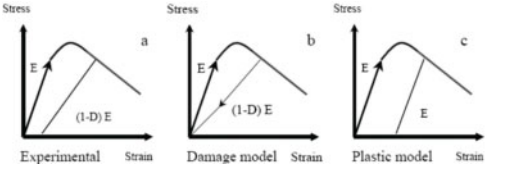

Figure 1. Elastic plastic damage law (Jason et al. 2004).

DOI 10.1201/9781003316404-30

The CDP model is combining the stress-strain curves in Figure 1b and c into Figure 1a so that we can better capture the constitutive behaviour of concrete. In SLS-design, compressive crushing of the concrete is generally not a problem and therefore the damage model for compression is excluded from the analyses described in this paper.

2.1 *Material constitutive behaviours*

The applied numerical models for the constituent material properties are described in this section

2.1.1 *Concrete model*

CDP describes the constitutive behaviour of concrete by introducing scalar damage variables. Both tensile and compressive response of concrete can be characterized by CDP, and the tensile response is depicted in Figure 2. Concrete behaviour in compression are not explained in this section due to investigated beams being within the elastic compression range.

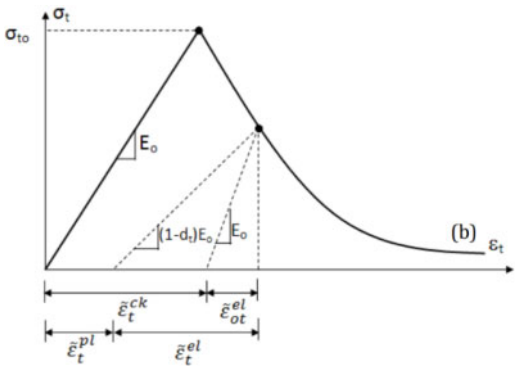

Figure 2. Behaviour of concrete under axial tension according to CDP (Abaqus User Manual 2014).

As shown in Figure 2, the unloading response of concrete specimen is weakened because the elastic stiffness of the material appears to be damaged or degraded. Damage associated with the failure mechanisms of the concrete (cracking and crushing) results in a reduction in the elastic stiffness. The CDP-model characterizes this by a scalar damage variable, d_t which can take values from zero (undamaged material) to one (fully damaged material). (Abaqus User Manual 2014). E_0 is the initial (undamaged) elastic stiffness of the material and $\tilde{\varepsilon}_t^{pl}$ and $\tilde{\varepsilon}_t^{in}$ are tensile plastic strain and inelastic strain respectively. The stress-strain relation under uniaxial tension is taken into account in Eq. (1).

$$\sigma_t = (1 - d_t) \cdot E_0 \cdot (\varepsilon_t - \tilde{\varepsilon}_t^{pl}) \tag{1}$$

A strain softening behaviour at the crack is assumed in the model. Thus, it is necessary to define the behaviour of plain concrete in tension for the CDP-model. ABAQUS allows the user to specify concrete

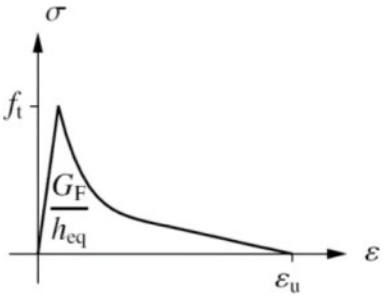

Figure 3. Hordijk softening curve (Hordijk & Dirk Arend 1991).

by post a failure stress-strain relation or by applying a fracture energy cracking criterion (Abaqus User Manual 2014) The former relation is used by the authors.

The stress strain relation for concrete in tension must be given to Abaqus in terms of the cracking strains, $\tilde{\varepsilon}_t^{ck}$, and corresponding yield stresses σ_{t0} which are determined from the nonlinear Hordijk curve (Hordijk, Dirk Arend. 1991). The exponential-type of softening diagram shown in Figure 3 will typically result in localized strains when the concrete in a structural member crack.

The area under the stress-strain curve should be equal to the fracture energy (G_f) divided by the equivalent length (h_{eq}) often called crack bandwidth. After complete softening i.e., when virtually no stresses are transmitted, the crack is said to be "fully open". The ultimate strain parameter in case of the Hordijk softening curve is given by

$$\varepsilon_u = 5.136 \frac{G_F}{h_{eq} f_t} \tag{2}$$

where f_t is the tensile strength of the concrete. The softening curve is given by

$$\sigma = \begin{cases} f_t \left(\left(1 + \left(c_1 \frac{\varepsilon^{cr}}{\varepsilon_u} \right)^3 \right) \exp\left(c_2 \frac{\varepsilon^{cr}}{\varepsilon_u} \right) \right) & 0 \le \varepsilon^{cr} \le \varepsilon_u \\ -\frac{\varepsilon^{cr}}{\varepsilon_u} \left(1 + c_1^3 \right) \exp(-c_2) & \\ 0 & \varepsilon^{cr} > \varepsilon_u \end{cases} \tag{3}$$

where c_1 and c_2 are parameters used to obtain the stress-crack width opening relation for concrete from deformation-controlled uniaxial tensile tests (Hordijk & Dirk Arend 1991). The recommended values are 3 and 6.93 respectively and are also applied in this study. The determination of the fracture energy G_f in tension is more complicated, and the authors have chosen this value to be as recommended by the Dutch guidelines (Hendriks 2017) and *fib* Model Code 2010 (fib 2013).

$$G_F = 0.073 f_{cm}^{0.18} \tag{4}$$

The tension softening data according to the Hordijk curve in Equation 3 are given to Abaqus in terms of

cracking strain $\tilde{\varepsilon}_t^{ck}$ and yield stress σ_{t0} as shown in Figure 2. When the unloading data are available, the data are provided to Abaqus in terms of tensile damage curves, $d_t - \tilde{\varepsilon}_t^{ck}$. Abaqus automatically converts the cracking strain values to plastic strain values using the relationship given by:

$$\tilde{\varepsilon}_t^{pl} = \tilde{\varepsilon}_t^{ck} - \frac{d_t}{(1-d_t)}\frac{\sigma_t}{E_0} \tag{5}$$

From this equation the effective tensile cohesion stress ($\bar{\sigma}_t$) determines the size of the yield (or failure) surface as:

$$\bar{\sigma}_t = \frac{\sigma_t}{(1-d_t)} = E_0(\varepsilon_t - \tilde{\varepsilon}_t^{pl}) \tag{6}$$

In Abaqus the parameters required to define the CDP-model consists of four constitutive parameters. First the angle of internal material friction of the concrete 'ψ' measured in the p-q plane at high confining pressure, and in this study, is chosen as recommended default value. The second parameter is the eccentricity ? which defines the rate at which the hyperbolic flow potential flow potential approaches its asymptote and is chosen as default value of 0.1. The third parameter is the ratio of initial biaxial compressive yield stress to initial uniaxial compressive yield stress, 'fb0/fc0', with a default value of 1.16. The fourth parameter is the ratio of the second stress invariant on the tensile meridian to the compressive meridian at initial yield with a default value of 2/3 (Abaqus User Manual 2014).

The parameter 'Kc' should be defined based on the full triaxial tests of concrete, moreover, a biaxial laboratory test is necessary to define the value of 'fb0/fc0'. This paper does not discuss the identification procedure for parameters 'ϵ', 'fb0/fc0', 'Kc' or 'ψ' because the test series that is in this study does not have such information. Therefore, default values have been chosen.

In nonlinear finite element programs, the material models softening behaviour and stiffness degradation can often lead to severe convergence difficulties. A common technique to overcome some of these difficulties is the use of a viscoplastic regularization of the constitutive equations, which causes the consistent tangent stiffness of the softening material to become positive for sufficiently small-time increments. The CDP-model in Abaqus can be regularized by using viscoelasticity to permit stresses to be outside of the yield surface. Using a small value for the viscosity parameter (μ) (small compared to the characteristic time increment) usually helps to improve the rate of convergence of the model in the softening regime, without compromising the results (Abaqus User Manual 2014). The viscosity value used by the authors in this work was chosen as 0 and 0.0001 which is shown to be sufficiently low to give realistically results (Demir et al. 2018). The plasticity damage parameters used by the authors are shown in Table 1.

Tension stiffening is implicitly modelled by the chosen tensile softening law and corresponding chosen mesh, thus causing localization of cracking strains in the tensile zone of the investigated beams for the concrete elements. Distance between localized cracking strains becomes analogous to a crack spacing. This in turn should result in steel strains varying between the crack spacing, having its maximum at a crack and its minimum between two consecutive cracks. This also means that tension stiffening should be accounted for without having to explicitly model the bond between concrete and steel.

3 PREDICTION OF CRACK WIDTHS

The crack width calculation methods according to EC2, MC2010 and the drafts for the new versions of EC2 are briefly highlighted in the following. Chosen values for the parameters used in the subsequent crack width calculates are also addressed.

3.1 *Eurocode 2 Part 1-1*

The method for calculation of crack widths applies the following equation:

$$w = S_{r,max}(\varepsilon_{sm} - \varepsilon_{cm}) \tag{7}$$

Where $S_{r,max}$ is the maximum crack spacing for a stabilized cracking stage expressed as:

$$S_{r,max} = k_3 c + k_1 k_2 k_4 \frac{\varphi}{\rho_{s,ef}} \tag{8}$$

Here $k_1 = 0.8$, $k_2 = 0.5$, $k_3 = 3.4$ and $k_4 = 0.425$ are chosen, while φ is the diameter of longitudinal reinforcement and $\rho_{s,ef}$ is the reinforcement ratio in the effective concrete tensile zone. The difference in mean strains is calculated according to:

$$(\varepsilon_{sm} - \varepsilon_{cm}) = \frac{\sigma_s - k_t \frac{fctm}{\rho_{s,ef}}\left(1 + \alpha_e \rho_{s,ef}\right)}{E_s} \geq 0.6\frac{\sigma_{sr}}{E_s} \tag{9}$$

where σ_s is the reinforcement stress, and $k_t$is dependent on load duration (short- or long-term loading) and varies from 0.4 to 0.6. The authors have chosen $k_t = 0.6$ due to the probable absence of creep and shrinkage in the experimental results and applies in general as a chosen value for the other codes as well. The ratio between steel and concrete Young's modules is defined as $\alpha_e = E_s/E_{cm}$ (Eurocode 2 Part 1-1, 2004).

Table 1. Plasticity damage parameters.

Ψ	E	fb0/fc0	Kc	μ
35	0.1	1.16	0.667	0 and 0.0001

3.2 *Model Code 2010*

The maximum calculated crack width at the height of the reinforcement is found by:

$$w = 2l_{s,max}(\varepsilon_{sm} - \varepsilon_{cm}) \tag{10}$$

when the term related to shrinkage strains is neglected. Here, $l_{s,max}$ denotes the length over which slip between concrete and steel is assumed to occur and is expressed by:

$$l_{s,max} = k \cdot c + \frac{1}{4}\frac{f_{ctm}}{\tau_{bms}}\frac{\varphi_s}{p_{s,ef}} \tag{11}$$

where $k = 1$ is an empirical parameter considering the influence of the concrete cover chosen according to the recommended value and c is the concrete cover. The mean bond strength between steel and concrete is chosen as $\tau_{bms} = 1.8f_{ctm}$. The relative mean strain in Equation 10 is the same as chosen in Equation 9 but the lower bound limits between the mean strains are different.

MC2010 allows for extrapolation of the crack width at the reinforcement height given in Equation 10 by a factor (h-x)/(d-x) where, h is cross-section height, x is the height of the compressive sone, and d is the effective height. This extrapolation is valid for cover up to 75mm. For larger covers a more detailed analysis is required and procedures based on fracture mechanics approach would be appropriate.

3.3 *Draft for the new Eurocode 2, 2022 (pr EN 1992-1-1)*

In the draft for the new Eurocode 2 the calculation of crack width is expressed as:

$$w_{k,cal} = k_w S_{rm,cal}(\varepsilon_{sm} - \varepsilon_{cm}) \tag{12}$$

where $k_w = 1.7$ is a factor converting the mean crack width into a calculated crack width and is chosen according to the recommended value. $S_{rm,cal}$ is the calculated mean crack spacing assumed to be valid for both initial cracking and a stabilized crack pattern.

For elements subjected to direct loads or subjected to imposed strains $\varepsilon_{sm} - \varepsilon_{cm}$ can be expressed as:

$$\varepsilon_{sm} - \varepsilon_{cm} = k_{1/r}\frac{\sigma_s - k_t\frac{fctm}{\rho_{s,ef}}\left(1 + \alpha_e\rho_{s,ef}\right)}{E_s} \geq 0.6\frac{\sigma_{sr}}{E_s} \tag{13}$$

Where $k_{1/r}$ is a coefficient to account for the increase of crack width due to curvature which is expressed as:

$$k_{1/r} = \frac{h - x}{h - a_{y.i} - x} \tag{14}$$

Here x is the distance to the neutral axis, and $a_{y.i}$ is the cover distance plus rebar size. The mean crack spacing is:

$$S_{r,m,cal} = 1.5c + \frac{k_{fl}k_b}{7.2} \cdot \frac{\varphi}{\rho_{p,ef}} \tag{15}$$

where c is cover to the longitudinal reinforcement, φ is bar diameter, $k_b = 0.9$ is a coefficient for bond properties for ordinary reinforcement chosen according to the recommended value and $k_{fl} = (h - h_{c,eff})/h$, where h is cross-section height and $h_{c,eff}$ is the effective tension area.

3.4 *NLFEA and codes*

EC2 and MC2010 both state that SLS verifications using NLFEA can be performed a posteriori. In the case of bending cracks, the crack opening (w) may be calculated according to Dutch guidelines (Hendriks 2017):

$$w = S_{r,max} \cdot \bar{\varepsilon_s} \tag{16}$$

Where $\bar{\varepsilon_s}$ is the mean strain value of the longitudinal reinforcement in the cracked zone obtained in the analysis and $S_{r,max}$ is the maximum crack spacing according to EC2.

4 EXPERIMENTAL TEST AND FEA MODELLING

4.1 *Hognestad beam tests, control of flexural cracking*

From the established database, the investigation carried out by Hognestad (1962) was chosen as appropriate for this paper. This experimental work involved 36 rectangular beams with a length of 3429 mm. Different parameters were chosen as major variables such as bar diameter, bar type, concrete strength, reinforcement ratio, beam width and depth and thickness of cover as shown in Table 2 (Hognestad 1962). All beams were loaded by twin-loads at the third points of the span. To prevent shear failures, the outer thirds were reinforced with ø10 stirrups. The beams examined in this study are No 31 and 32, with respective properties given in Table 3. The different parameter variables shown in Table 2 are included to highlight the extensive work done by Hognestad and are relevant for further work.

Table 2. Parameter variations done by Hognestad.

Beams No.	Major Variable	Description
1–4	Bar diameter	Size and number of rebars
5–7	Bar diameter	Size and number of rebars
8–10	Bar diameter	Size and number of rebars
11–12	Bar diameter	Size and number of rebars
13–16	Bar diameter	Size and number of rebars
17–20	Bar diameter	Size and number of rebars
21–24	Beam width	Size and number of rebars
25–28	Beam depth	Size and number of rebars
29–32	Concrete cover	horizontal cover
33–36	Concrete cover	vertical and horizontal cover

* Both compressive and tensile concrete strength varied for the test series (Hognestad 1962).

Table 3. Geometrical and material properties for Beam No 31 and 32.

Description	mm	Description	MPa
Beam height*	406	fck*	25,1
Beam width*	203	fct*	2,57
Cover vertical B31	63	Es*	200.000
Cover vertical B32	112	Ec*	31.504
Cover horizontal*	25		
Effective depth B31	322		
Effective depth B32	294.5		
Beam length*	3429		
Bar size*	22		
Number of bars*	2		

* Properties shared by both beams No 31 and 32.

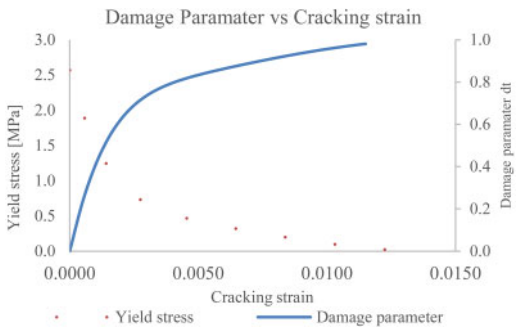

Figure 4. Softening branch of concrete in tension with corresponding damage parameter development applied by Abaqus.

Table 4. Stress-strain values for reinforcement and steel plates.

Yield Stress (σ_t) MPa	Plastic Strain $\tilde{\varepsilon}^{pl}$
Reinforcement:	
575*	0.0
Steel plates:	
275*	0.0

* Both steel plates and reinforcement never reach yielding during the analysis and plastic strains are therefore not calculated

4.2 *Finite element modelling of the RC beams*

To develop the FE models of the RC beams, steel loading- and support plates as well as the concrete cross-section were modelled using 3D brick elements. The FE models thus consist of three types of materials (concrete, steel plate, reinforcement). The embedded reinforcement technique available in ABAQUS is also used. The beams are reinforced with 22 mm rebar diameters with either 84 mm or 122.5mm distance from the outermost surface to the centroid of the reinforcement.

The elements chosen for concrete and steel plates in Abaqus is C3D20R quadratic brick elements with reduced integration (20 nodes and 8 integration points). The element size is approximately 20x20x20 mm and chosen in accordance with Dutch guidelines (Hendriks 2017) maximum element size for NLFEA. For the longitudinal reinforcement wire elements each with a length of 20 mm is used. The loading of both beams are displacement controlled.

There is a mesh sensitivity problem in cases with little or no reinforcement with the specification of a post failure stress-strain relation, in the sense that the finite element predictions do not converge to a unique solution as the mesh is refined because mesh refinement leads to narrower crack bands. In these beam models a post failure material behaviour as explained earlier with tension stiffening derived from Hordijk softening curve is applied and the cracking failure are distributed evenly and results in additional cracks and mesh sensitivity analysis with other element sizes is not performed.

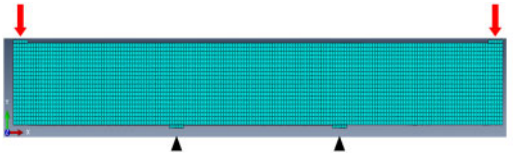

Figure 5. Model of Hognestad Beam in Abaqus.

5 RESULTS

5.1 *Load displacement behaviour*

The load displacement curves were not reported by Hognestad and therefore the FEA load-displacement is used as an indicator for crack development and used to compare when cracking occurs. Also, some sensitivity checks applying various values for the previously discussed viscosity parameter are performed. Viscosity parameters equal to 0 and 0.0001 were used, and from 5.2 we can observe that for beam No. 31 that when initial cracking occurs at approximately 20 kN loading there is a slight difference between the two solutions. This is due to that the viscosity parameter greater than 0 allows for stresses outside the yield surface but provides accurate enough results. For beam No. 32 the Viscosity parameter of 0 are not done due to the iterative process and length of the analysis required.

5.2 *Experimental crack widths*

From the Hognestad beam tests measured surface crack widths at both the height of the steel centroid and concrete top face are reported. The results for the selected beams are given in 5.3. From the measured crack widths, we notice that the crack widths at the height of reinforcement are similar regardless of concrete cover.

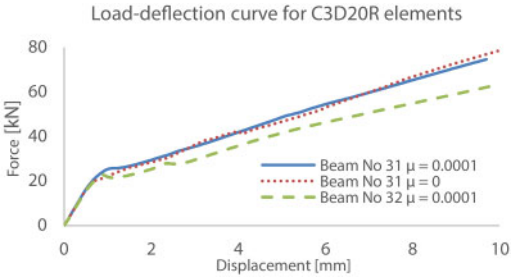

Figure 6. Load deflection curve for different viscosity parameter.

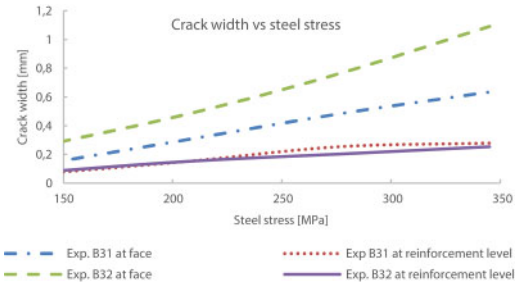

Figure 7. Experimental maximum crack widths vs steel stresses for beam No. 31 and No. 32 (Hognestad 1962).

5.3 *Maximum crack width predicted by design codes*

The predicted maximum crack widths according to EC2, MC2010 and the draft for new EC2 from equations 7,10 and 12 are compared in Figure 8.

It can be noted that for both beams the estimated crack widths are conservative at the height of reinforcement but underestimated at the outermost concrete face for EC2 and the draft for new EC2. MC2010 predict the crack width at the outermost concrete face to a good extent for 62 mm cover but underestimate it for 112 mm cover. The extrapolation of the results to get the crack width at the outermost concrete face are not valid for a larger cover than 75mm but are chosen to be included here.

The new term ($k_{1/r}$) accounting for the curvature in the new EC2 looks to provide a better result for the crack width at increased steel stresses beyond 250 MPa for both beams than the current EC2.

5.4 *Calculations of crack widths combining NLFEA and EC2*

The maximum crack width is calculated from Equation 16. Mean steel strains ($\bar{\varepsilon}_s$) for Beam No. 31 and 32 are extracted from the NLFEA. The maximum crack spacing ($S_{r,max}$) is calculated from equation 8 in accordance with EC2. In addition, the measured maximum spacing between the cracks in the constant moment zone from the Abaqus models at the stabilized cracking stage is also used (steel stress close to 350MPa).

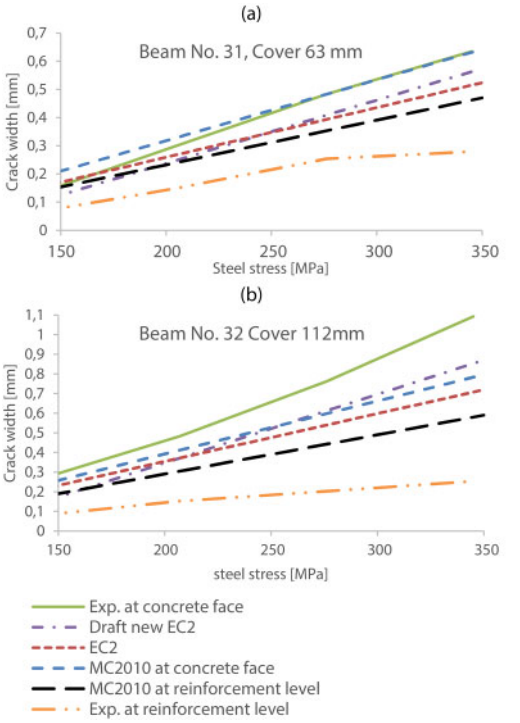

Figure 8. Crack widths predicted by design codes, (a) Beam No. 31, (b) Beam No. 32.

From Figure 9 we can determine the maximum crack spacings from where we have a stabilized cracking pattern at $\sigma_s = 350$ MPa, to (a) $S_{r,max} = 240$ mm and (b) $S_{r,max} = 300$ mm.

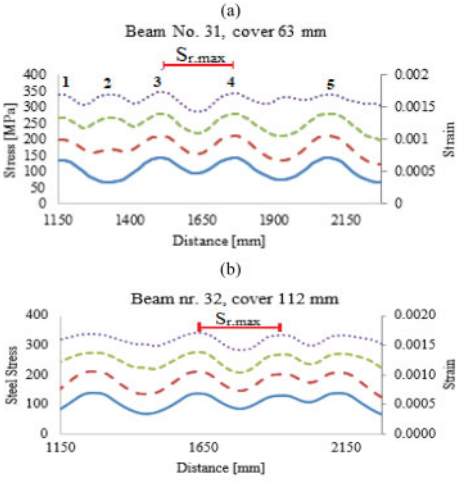

Figure 9. Steel stress levels and corresponding strains along the rebar length in the cracked concrete zone (constant moment), (a) Beam No. 31 numbers 1-5 indicate the localization of cracking strains in Figure 13, (b) Beam No. 32.

From Figure 10 the method based on extracting mean steel strains from the NLFEA and using the EC2 formulation for $S_{r,max}$ and the maximum crack spacing from the analysis shown in Figure 9 to calculate the crack widths at the reinforcement height are conservative. On the other hand, the EC2 formulation for maximum crack spacing fits better at the outmost concrete face than the maximum crack spacing from the analysis.

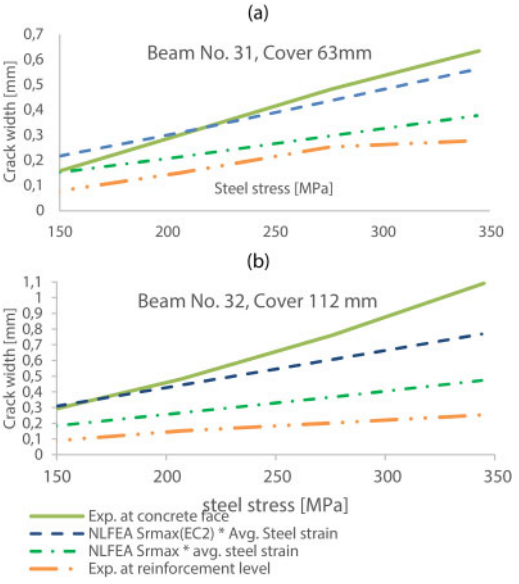

Figure 10. Crack widths estimated by extracting steel strains from NLFEA, (a) Beam No. 31, (b) Beam No. 32.

5.5 *Crack width determined by the Concrete Damage Plasticity model*

From the results in Abaqus the cracking strains are found meaning we can determine the crack width as:

$$w = \varepsilon^{cr} \cdot h_{eq} \tag{17}$$

The cracks localize within the brick elements, and at the top face of the beam the crack widths vary over the width of the beam. The crack widths are calculated by selecting the cracked elements across the beam width and using average cracking strain ε^{cr} multiplied with the crack band width (h_{eq}) which is an essential parameter in constitutive models that describe the softening stress-strain relationship. The preferred method is a method based on the initial direction of the crack and the element dimensions (Hendriks 2017). For both beams the length of the crack band width is 20mm. The development of the crack width using this method is shown in Figure 11. The crack localizations are visualized in 6.

Crack 1 in Figure 11 is selected representing the maximum crack width for both beams and compared

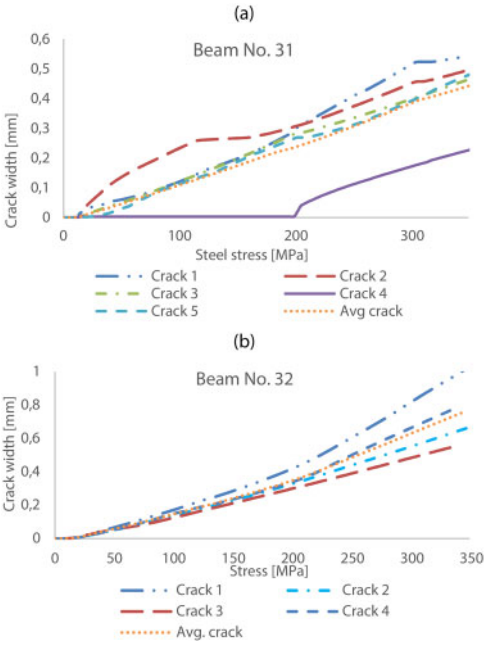

Figure 11. Crack widths of major cracks in the constant moment zone estimated by NLFEA, (a) Beam No. 31, (b) Beam No. 32.

to the reported experimental crack width values in Figure 12.

It is observed that the NLFEA with CDP-model can accurately predict the crack width at the concrete face for the two experimental beams.

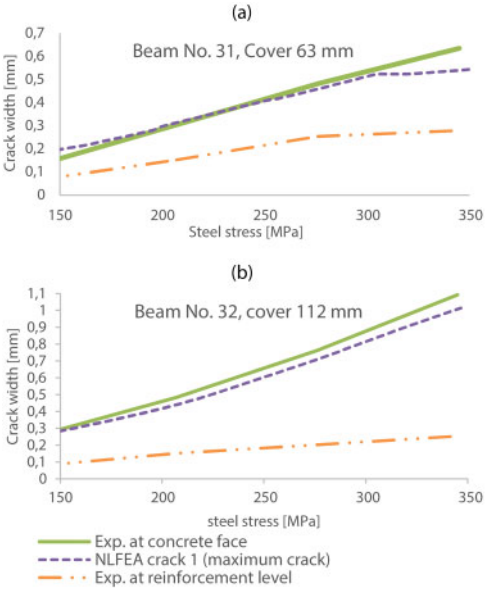

Figure 12. Maximum crack widths estimated by NLFEA CDP-model vs experimental values, (a) Beam No. 31, (b) Beam No. 32.

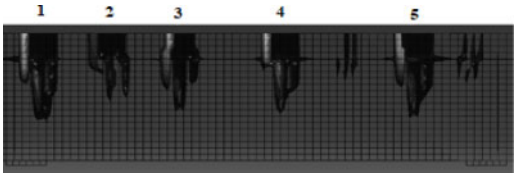

Figure 13. Visualization of localized cracking strains in between the supports for Beam No. 31 at $\sigma_{sr} = 350MPa$.

6 DISCUSSION

By applying the CDP-model with embedded reinforcement (no-slip) and calculating the crack width directly (Equation 18) by the cracking strain and the selected bandwidth as shown in Figure 14, we were able to obtain good crack width predictions of the reported experimental results at the outer most concrete face. Using the Dutch guidelines (Equation 16) with maximum crack spacing ($S_{r,max}$) defined in EC2 (Equation 8) provided also good agreement for beam No. 31 with cover 63 mm, while for beam no. 32 with cover 112 mm the results are to the unconservative side at the outermost concrete face. One reason looks to be that the maximum crack spacing ($S_{r,max}$) in EC2 does not fully consider the curvature effect for beams in bending and the impact of large concrete covers do not seem to be fully accounted for in the current code.

EC2 underestimate the maximum crack width at the outermost concrete face. In fact, it is observed that the underestimation is increasing for larger concrete cover. This seems to be addressed better in the draft for the new EC2 which introduces a coefficient ($k_{1/r}$) to account for increased crack widths due to the curvature from bending. However, it is still underestimating the crack widths at the outermost concrete face, but the results look to be more consistent in comparison with the current EC2. The need for this coefficient for concrete beams subjected to pure bending is supported by the observed results shown in Figure 7 and 14, as it is noticed that both beams have quite similar measured experimental crack widths at the reinforcement level.

MC2010 predict the crack width at the outermost concrete face for beam No. 31 to a very good extent by extrapolating the calculated crack width at reinforcement level, while being conservative at the reinforcement level. The corresponding result for Beam No. 32 by using MC2010 might be considered invalid since the distance from the reinforcement level to the outmost concrete face is larger than 75 mm. It is not clear to the first author how the code accounts for this except stating the following: *"For larger concrete cover a more detailed analysis is required. Procedures based on the fracture mechanics approach would be appropriate"*. However, it seems that methods like the CDP-model are applicable.

From the investigated beams it can be noted that a pivotal question has risen. At which location should

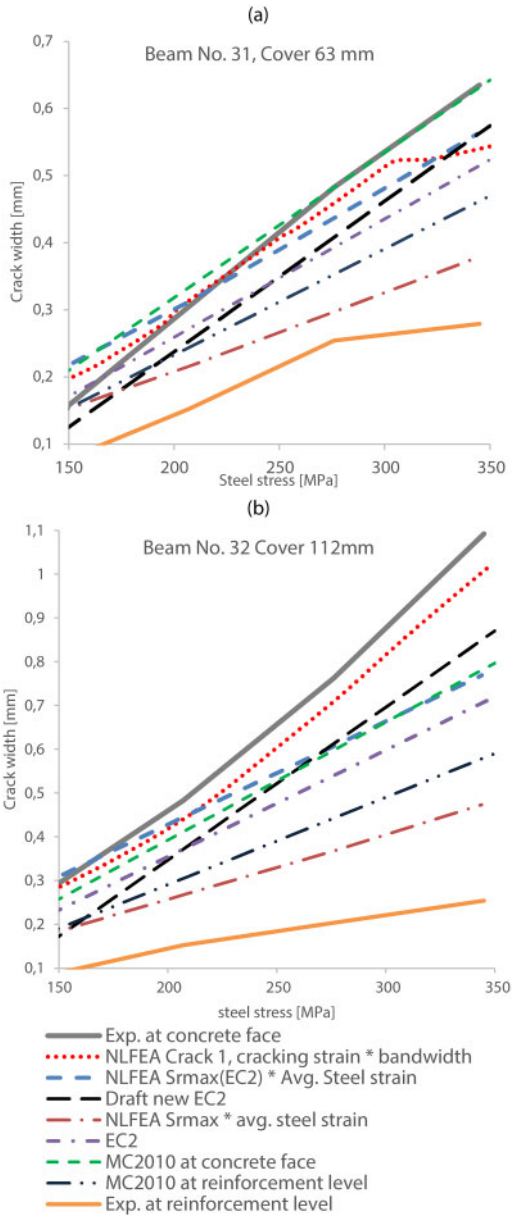

Figure 14. Crack widths vs steel stress for different approaches, (a) Beam No. 31, (b) Beam No. 32.

the maximum crack width be determined? The term accounting for the curvature in the new EC2 ($k_{1/r}$) is logical, but especially for beams with large concrete cover this gives large crack widths at outermost concrete face. This increase in calculated crack width might have large economic consequences if not the allowed crack limits in the codes are adjusted to this increase. A relevant observation for this discussion is that both beams have quite similar measured experimental crack widths at the reinforcement level that we want to protect with a concrete cover.

7 CONCLUSIONS

In this paper NLFEA with the concrete damage plasticity (CDP) model has been used to calculate the maximum crack widths in beams. The results have been compared to experimental values and results from various analytical prediction models. The results suggest that the following conclusion can be drawn:

1. 3D NLFEA analysis with the CDP model and embedded reinforcement is used to calculate the maximum crack width by multiplying the largest average cracking strain at the concrete face through the width of the beam with the selected bandwidth (Equation 18). The resulting crack widths gave predictions in good agreement with the experimental values at the outer most concrete face regardless of the cover size. This suggests that this method take the effect of cover and curvature due to bending into account better than the other NLFEA solutions and the analytical methods in the codes.
2. EC2 gave conservative results for the maximum crack width at the reinforcement level but underestimate the crack width at the outermost concrete face for the investigated beams. This suggest that the current EC2 do not correctly account for the concrete cover and the curvature effect.
3. MC2010 gave conservative results for the maximum crack width at the reinforcement level for both beams. While it gave good predictions at the experimental values at the outermost concrete face for a cover of 63 mm, the prediction was poor for cover size 112 mm. This cover size is greater than the allowed value of 75 mm and thereby clearly shows the limited validity range for beams subjected to bending in MC2010.
4. Calculating the maximum crackwidth from the draft of the new EC2, accounting for the increase in curvature by the factor $k_{1/r}$ gives better agreement than the current EC2 for crackwidth at the outermost concrete surface for increased steel stresses but is still slightly to the unconservative side. This suggests that the introduction of a curvature effect is a more correct solution for beams in bending, but this is based on only two examined beams.
5. Crackwidth calculations based on extracting the average steel strains from the NLFEA with a maximum crack spacing have been performed using two approaches:
   (a) With $S_{r,max}$ from EC2: Good agreement with crack widths at the outermost concrete face was achieved for beam no. 31 but were unconservative for beam no. 32. This suggest that the maximum crack spacing in EC2 do not fully account for the effect of large concrete covers.
   (b) The approach with $S_{r,max}$ extracted directly from the NLFEA is considerably underestimating the crackwidth at the outermost concrete face but is conservative at the reinforcement level.
6. From the conclusions in 1-5 the following can be derived:
   - Predicting crack widths at the outer most concrete face 3D NLFEA with CDP-model using cracking strains and a selected bandwidth (Equation 18) have no visible cover restrictions and gave the best results for the methods involving NLFEA.
   - From the applied codes, the draft for new EC2 seems best suited for a general crack width estimation regardless of concrete cover for beams subjected to bending.

8 FURTHER WORK

The authors are currently establishing a larger crack width database including a large number of experimental studies. Some of these will be investigated further with NLFEA to supply more raw data for recommendations on different solutions for better crack width prediction in beams subjected to bending with large concrete covers.

REFERENCES

Demir, A et al. 2018. "Effect of viscosity parameter on the numerical simulation of reinforced concrete deep beam behavior." *The Online Journal of Science and Technology*

Hordijk, Dirk Arend. 1991. "Local Approach to Fatigue of Concrete." *Delft University of Technology, The Netherlands*.

Hognestad, E. 1961 "High Strength Bars as Concrete Reinforcement Part 1. Introduction to a Series of Experimental Reports" *Journal of the PCA Research and Development Laboratories September 1961*

Hognestad, E. 1962 "High Strength Bars as Concrete Reinforcement Part 2: Control of Flexural Cracking" *Journal of the PCA Research and Development Laboratories September 1962*

M.A.N Hendriks, A. de Boer, B. Belletti, "Guidelines for Nonlinear Finite Element Analysis of Concrete Structures", *Rijkswaterstaat Centre for infrastructure, Report RTD: 1016-1:2017, 2017.*

Basteskår M, Engen M, Kanstad T, Fosså KT. *"A review of literature and code requirements for the crack width limitations for design of concrete structures in serviceability limit states" Structural Concrete. 2019;1.11.*

Basteskår, M., Engen, M., Kanstad, T., Johansen, H., Fosså, K. *"Serviceability limit state design of large concrete structures: Impact on reinforcement amounts and consequences of design code ambiguity." Engineering structures* 2019; Vol. 201.

Lubler, J., J. Oliver, S. Oller, and E. Oate, *"A Plastic-Damage Model for Concrete,"* International Journal of Solids and Structures, vol. 25, no.3, pp. 229–326, 1989.

Lee, J., and G. L. Fenves, *"Plastic-Damage Model for Cyclic Loading of Concrete Structures,"* Journal of Engineering Mechanics, vol. 124, no.8, pp. 892–900, 1998.

Tan, Reignard. 2019 "Consistent crack width calculation methods for reinforced concrete elements to 1D and 2D stress states A mixed experimental, numerical and analytical approach" Doctoral thesis, Norwegian University of Science and Technology.